

SIMULATION AND EXPERIMENTAL STUDIES OF 699.3 MHZ RF-STRUCTURES FOR THE ELECTRON PULSE STRETCHER

I.M.Karnaukhov, I.I.Koba, Yu.P.Popkov,
Yu.N.Telegin, N.A.Trushkin, G.V.Tsepilov
Institute of Physics and Technology,
310108, Kharkov, USSR
A.G.Abramov, A.G.Daikovsky, A.D.Ryabov
IHEP, 142284, Serpukhov, USSR

Abstract: Cavity simulations for several types of RF-structures have been made using computer codes PRUD-0 and PRUD. A 5-cell Ω -structure having the lowest parasitic impedances was chosen for modelling and further studies. The influence of coupling slots on structure properties was studied on model cavities.

Introduction

The project of upgrading the Kharkov 2 GeV electron linac includes the construction of the pulse stretcher and storage ring (PSSR) [1], which is designed to operate in the energy range (0.5-3.0) GeV at peak circulating currents up to 150 mA and average extracted currents up to 30 μ A. Beam energy losses in the ring will be compensated by an RF-system using six 5-cell 699.3 MHz accelerating cavities. A multibunch operation of the PSSR imposes stringent restrictions on impedances of higher order modes (HOMs) of the RF-cavities, because the beam interaction with narrow-band cavity resonances can drive coupled bunch oscillations and thus result in the beam loss.

In order to choose an appropriate structure and to optimize the cell shape, a series of computer simulations and cold tests with model cavities were performed. In this paper we report the simulation results for several types of RF-structures, obtained with the 2D finite-element computer codes PRUD [2] and PRUD-0 [3], together with the experimental data from cold tests of the Ω -shaped model structure.

Computer simulation and calculation of the electromagnetic properties

The following three types of RF-structures were simulated:

- structure with a cell of the "pill-box" shape (structure A);
- Ω -structure;
- biperiodic, on-axis coupled structure (ACS).

The cell profiles (a half of the structure period) are presented in Fig.1. Following beam dynamics calculations, the aperture radius, α was fixed to be 50 mm, and the web width, δ was chosen so that proper web cooling and rigidity of the design should be provided.

The fitting of the cell dimensions to the required fundamental frequency- f_0 , optimization of the cell shape and the calculation of RF-properties for axisymmetric (monopole) cavity modes (TM_0 -like and TE_0 -like) were performed using the computer code PRUD-0. It was found that the tilting angle θ variations in a wide range and the replacement of the tilt by a spherical surface leads to 0.5 % changes in shunt impedances (including the

fundamental TM_{010} mode) and to negligible shifts (less than 0.1 MHz) of HOM eigenfrequencies.

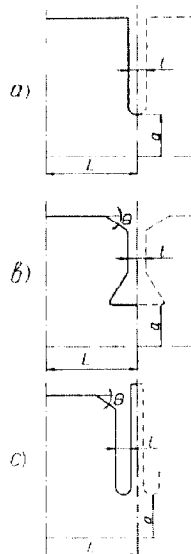


Fig.1 Cell profiles (a half of the structure period):
a) "pill-box";
b) Ω -structure;
c) ACS.

The calculated eigenfrequencies and factors R_1^H/Q_1 for TM_0 -modes below the cut-off frequency of the vacuum pipe ($f_c = 2.295$ GHz) are listed in table 1. E and M in the first column correspond to Dirichlet and Neumann boundary conditions, respectively, as applied to a half-cell.

Table 1

Boundary conditions	Cavity mode	A		Ω -structure		ACS	
		f_1 , MHz	R_1^H/Q_1 , Ω/μ	f_1 , MHz	R_1^H/Q_1 , Ω/μ	f_1 , MHz	R_1^H/Q_1 , Ω/μ
EM	TM_{010}	699.3	669	699.3	664	699.3	727
ME	TM_{010}^C	-	-	-	-	699.3	81
ME	TM_{011}	1026.9	372	1050.3	234	1170.6	250
EM	TM_{020}	1609.2	41	1736.5	38	1609.9	34
ME	TM_{020}^C	-	-	-	-	1667.6	37
EM	TM_{012}	1682.1	14	1741.1	5	1970.5	33
ME	TM_{021}	1758.5	177	1986.1	74	1893.4	117
EM	TM_{022}	2247.9	92	-	-	-	-
$\Sigma R_1^H/Q_1, (f_1 < f_c)$			696		351		552
$(\Sigma R_1^H/Q_1)/R_1^H/Q_1$			1.04		0.41		0.76

The table also lists the sums $\sum_i R_i^H/Q_i$ over the modes with f_i/f_c , and the ratios of these sums to the R^H/Q -values for the fundamental mode. It is seen that the Ω -structure has the highest shunt impedance of the operating mode and the lowest HOM impedances, so this structure seems a most favourable candidate for the PSSR accelerating cavity. Unfortunately, it has the lowest intercell coupling factor ($k_1 = 0.24$) and needs inductive coupling slots between neighbouring cells, which break the cylindrical symmetry of the structure and cannot be considered in 2D-calculations.

For dipole HEM_1 -modes, the transverse beam-cavity interaction plays a dominant role. This interaction can be described in terms of the transverse coupling impedance R^\perp which is related to the longitudinal one by the expression [4]:

$$R^\perp/Q = (1/kr)^2 R^H/Q, \quad (1)$$

where $k = \omega/c$ is the wave number, and r is the distance of the field integration path from the structure axis. As seen from expression (1), the transverse impedance is calculated from the off-axis field. In this work r was chosen to be 2.5 cm. The eigenfrequencies and R_i^H/Q_i values for HEM_1 -modes calculated by the PRUD code are listed in table 2. The mode classification given in the tables is based on commonly accepted notations for "pill-box" cavity modes. The symbols EH and HE are adopted for the dipole modes with a dominant electric or a magnetic field on the structure axis, respectively.

Table 2

Boundary conditions	Cavity mode	A		Ω -structure		ACS	
		f_1 , MHz	R_1^H/Q_1 , Ω/m	f_1 , MHz	R_1^H/Q_1 , Ω/m	f_1 , MHz	R_1^H/Q_1 , Ω/m
ME	EH_{110}^c	-	-	-	-	922.8	4.4
ME	HE_{111}	911.6	1.8	1001.4	3.3	1017.4	21.9
EM	EH_{110}	1044.8	156.6	1122.2	140.8	1056.7	221.1
ME	EH_{111}	1311.0	193.9	1387.1	169.7	1401.1	138.6
EM	HE_{112}	1422.6	8.1	1659.0	2.9	1572.0	16.4
ME	HE_{121}	1688.0	0.1	1796.8	0.4	1722.7	$0.5 \cdot 10^{-2}$
ME	EH_{120}^c	-	-	-	-	1851.9	32.0
EM	EH_{112}	1731.0	18.8	1803.2	9.3	1933.0	2.3

As it follows from the table, the Ω -structure appears still preferable to the other two structures, though its advantage with respect to the transverse beam-cavity interaction is not so evident.

The detailed description of cavity simulations can be found in [5].

Cold tests of the model Ω -cavities

The structure with an Ω -shaped cell was chosen for modelling and cold tests as a most promising accelerating structure for the PSSR. Two full-scale structure assemblies were studied:

- i) the single cell with two half-cells terminated by conductive end plates (see Fig.2);
- ii) two coupled cells with conductive plates in the irises of the end webs.

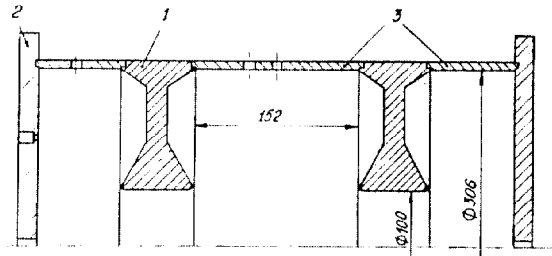


Fig.2 The model structure assembly: 1 - web; 2 - end plate; 3 - ring.

The webs, end plates were machined from refined copper, while the rings (cylindrical parts of the cells) were fabricated from steel and then electroplated with copper. The structures were assembled using indium seals to provide RF-contacts between different parts of the cell.

In the first step, the 721.3 MHz axisymmetrical structure (without coupling slots) was studied in order to compare experimental data with finite element code simulations. The frequency was chosen to be 3% higher than the operating frequency so as to attain the latter after cutting coupling slots.

Resonant frequencies and Q -values were measured by a network analyzer, connected to a pickup coupling loop ('on passage' method). The electric and magnetic field distributions were measured by a perturbation technique. The experimental equipment and measuring techniques have been described in [6]. The HOMs with high impedances predicted by calculations (see tables 1 and 2) were examined more precisely. The measured resonant frequencies, Q -values and R/Q -factors for fundamental and three most dangerous HOMs are listed in table 3 together with the calculated values. Triple modes with 0, $\pi/2$, π phase shifts per cell were observed for TM_{010} and EH_{110} modes, while only $\pi/2$, π -modes could be studied in the given structure assemblies for TM_{011} -like and EH_{111} -like cavity modes.

Table 3

Mode	Phase shift	f , MHz		$Q \cdot 10^{-4}$		R/Q , Ω/m	
		calc.	exp.	calc.	exp.	calc.	exp.
TM_{010}	0	719.2	719.2	3.4	2.4		
	$\pi/2$	720.3	720.1	3.4	2.4		
	π	721.3	721.3	3.4	2.4	850	908
TM_{011}	$\pi/2$	1057.1	1057.0	2.8	2.4		
	π	1055.9	1055.5	2.8	2.4	268	247
EH_{110}	0	1136.2	1167.0	4.4	2.9		
	$\pi/2$		1158.2		2.5		
	π	1122.2	1150.1	4.0	2.6	141	200
EH_{111}	$\pi/2$		1371.8		2.1		
	π	1387.1	1401.3	3.8	3.0	170	170

As it follows from the analysis of the data given in the table, the measured eigenfrequencies and R/Q -factors for monopole modes are in agree-

ment with the calculated ones. The difference in the R/Q factor for the operating TM_{010} mode must be attributed to the field distortion by the driving loop. For dipole modes, the calculated parameters have been taken for the 699.3 MHz structure, so here only qualitative agreement can be anticipated. Discrepancy between the calculated and measured Q-values for all modes studied is explained by a rather high degree of surface roughness of the model cells, especially of their electroplated parts (rings).

In the second step, the RF-characteristics of the Ω -structure were studied as functions of the coupling slot angle α in the range of 0° - 45° . We used only the first type of the structure assembly (i) which retained periodicity after cutting the coupling slots.

Fig.3 illustrates the transformation of the dispersion branch of the fundamental mode from the forward wave type into the backward wave type (in the travelling wave presentation), while the coupling slot angle increases from 0° to 20° . The intercell coupling factor, calculated from these data, is presented as a function of α in Fig.4 together with the analytical cal-

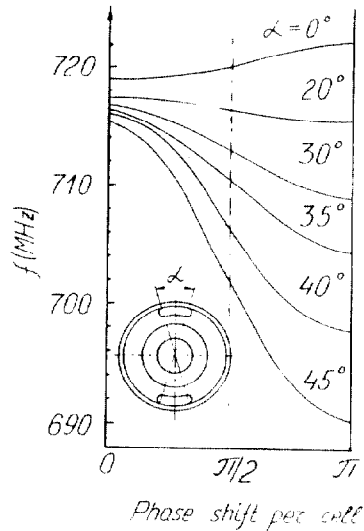


Fig.3 Dispersion curves for different slot angles.

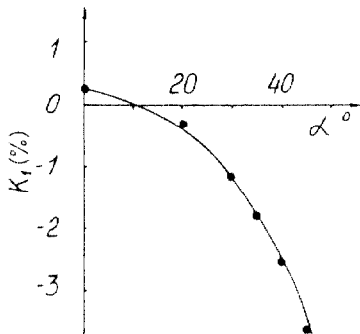


Fig.4 The coupling factor as a function of the coupling slot angle. Points: measurement, solid line: calculation.

culations made by the method described in [7]. The experimental errors are within point size. Good agreement between experiment and calculations is seen, while the estimated accuracy of the calculation method is 10%.

The measurements have also shown that the dipole modes split into two branches, as the slot angle increases, due to two possible orientations of the mode symmetries with respect to the slots. Frequency shifts caused by slot cutting depend on the relative orientations of the slots on opposite webs. The present results have been taken for the case when the angle between the slots in the neighbouring webs is 90° .

The slot cutting reduces shunt impedances of the fundamental and higher order modes. The measurements have shown that the shunt impedance of the operating mode is reduced by 6% for the structure with $\alpha = 40^\circ$, while the shunt impedance of the EH_{110} mode essentially decreases and is only a half of that for the structure without slots.

Conclusion

The computer simulations of several types of RF-structures have shown that the cavity with Ω -shaped cells is the most favourable candidate for the PSSR accelerating cavity because it has the lowest HOM impedances. Cold tests of the model Ω -structures support the calculation results and give the necessary basis for designing a full-scale 5-cell model cavity.

References

- [1]. V.F. Boldyshev et al., The Kharkov 2 GeV electron beam stretcher-storage ring (in Russian), in Proc. XIII Int. Conf. on High Energy Accelerators. Novosibirsk, Nauka publ., 1987, pp. 300-302.
- [2]. A.G. Daikovskiy, et al., PRUD-code for calculation of non-symmetric modes in axial symmetric cavity. Part. Accel., v.12, 1982, p.59-64.
- [3]. A.G. Abramov, et al., PRUD-0 program pack for calculations of accelerating structures (in Russian), Preprint IHEP EB-3 DMVT, Serpukhov, 1983.
- [4]. R. Klatt and T. Weiland. Comparison of six accelerating cavities with respect to collective effects. DESY Preprint M-84-06, 1984.
- [5]. I.M. Karnaukhov et al. Calculations of the electromagnetic parameters and the choice of RF-structure for the pulse stretcher and storage ring (in Russian), Preprint KhFTI-89-6, 1989, Moscow, TsNITIAI publ.
- [6]. I.I. Koba et al. Studies of the electromagnetic properties of Ω -shaped model cavities (in Russian), Preprint KhFTI-90-17, 1990, Moscow, TsNITIAI publ.
- [7]. V.L. Bukharin, et al., Designing of biperiodic accelerating structures. (in Russian), In collection: Linejnye uskoriteli, MIFI, Moscow, Energoatomizdat, 1989, pp. 13-18.